DESIGN AND EXPERIMENTAL STUDY OF A SOIL PICKUP AND SEPARATION DEVICE FOR AN AUTOMATIC FLOWER TRANSPLANTER
/
花卉自动移栽机取分土装置设计与试验研究

Xiang ZOU[1)], Lihua WEI*[1,2)], Denghui ZHAO[1)], Jian KANG[1)], Xiaohu BAI[1,2)] and Subo TIAN*[1,2)]
[1)]College of Engineering, Shenyang Agricultural University, Shenyang/ China;
[2)]Key Laboratory of Agricultural Equipment for Horticultural Crops, Ministry of Agriculture and Rural Affairs, Shenyang/ China.
Corresponding authors: Lihua Wei, Tel:13386825657; E-mail: weilihua@syau.edu.cn;
Subo Tian, Tel:13940428180; E-mail: tiansubo@syau.edu.cn.
DOI: https://doi.org/10.35633/inmateh-79-99

***Keywords:** flower transplanter; soil pickup and separation device; operating parameter optimization; discrete element simulation; Box-Behnken design; performance validation*

ABSTRACT
To enable automatic and precise flower transplanting, a soil pickup and separation device was designed for substrate filling in greenhouse flower transplanting operations. The soil-conveying mechanism of the soil pickup auger was analyzed through theoretical analysis and discrete element simulation. Taking the soil pickup quantity and its coefficient of variation as the evaluation indices, the effects of auger rotational speed, soil penetration depth, and pitch were investigated and optimized using Box-Behnken response surface methodology. The simulation results showed that the optimal operating parameters were an auger rotational speed of 115.7 rpm, a soil penetration depth of 39.28 mm, and a pitch of 149.26 mm. Based on the optimized parameters, a prototype was fabricated and field tests were conducted. The measured soil pickup quantity was 4.13 kg, and the corresponding coefficient of variation was 1.44%, with relative errors of 3.05% and 4.00%, respectively, compared with the simulation results. The validation results demonstrated that the device operated stably and could achieve accurate and efficient substrate filling.

摘要
为实现花卉移栽过程的自动化与精准化，针对温室环境下花卉自动移栽机的作业需求，本文设计了一种用于软质花盆基质填充的取分土装置。结合理论分析与离散元仿真明确取土搅龙推土机理，以取土量及变异系数为指标，用 Box-Behnken 响应面法优化转速、入土深度和螺距。仿真结果表明，当转速为 115.7 r·min⁻¹、入土深度为 39.28 mm、螺距为 149.26 mm 时，取土性能最优。基于优化结果试制样机并开展田间试验，实际取土量为 4.13 kg，变异系数为 1.44%，与仿真预测值的相对误差分别为 3.05%与 4.00%。试验结果表明，该装置结构合理、工作稳定，可实现花盆基质的精准高效填充。

INTRODUCTION
The floral industry is a high-value sector of global agricultural trade. Driven by emerging markets and consumption upgrades, global flower demand continues to grow—the market exceeded $51.16 billion in 2024. As a major producer and consumer, China's floral exports reached $516 million in 2024, a year-on-year increase of 17.78% *(Gu et al., 2025)*. Against this backdrop, the comprehensive mechanization of flower production is not only crucial for enhancing the competitiveness of the flower industry and supporting its sustainable development, but also a key step in promoting rural revitalization and achieving agricultural modernization *(Cheng et al., 2023)*.

Flower transplanting primarily involves two core steps: growing medium filling and seedling planting. Growing medium filling is a prerequisite that directly affects operational efficiency and quality. However, it remains largely manual in China, resulting in high labor intensity and inconsistent quality, and making it difficult to meet the demands of large-scale production *(Zhou et al., 2018)*. Although some studies have addressed matrix filling mechanisms *(Minglani et al., 2021, Xu et al., 2020, He et al.,2023)* and transplanting apparatus optimization *(Zhao et al., 2020, Zhao et al., 2022, Tian et al., 2022, Tian et al.,2023, Ji et al., 2022, Tong et al., 2024, Hu et al., 2022)*, most focus on single functional modules or theoretical simulation analyses. There is still a lack of integrated soil pickup and separation devices specifically designed for automatic transplanting on greenhouse ridges, as well as systematic experimental studies of their operating performance and parameter effects.

Moreover, existing soil pickup devices often perform poorly under variable field conditions, such as uneven ridge surfaces and differences in soil properties, resulting in fluctuations in soil pickup quantity and filling uniformity. To address these challenges, this study develops an integrated soil pickup and separation device, optimizes its operating parameters using EDEM simulation and response surface methodology, and validates its performance through field tests. The aim is to provide a reliable and precise soil-handling solution for automatic flower transplanting and to support the development of more efficient, stable, and intelligent transplanting equipment.

MATERIALS AND METHODS

Structure and Working Principle

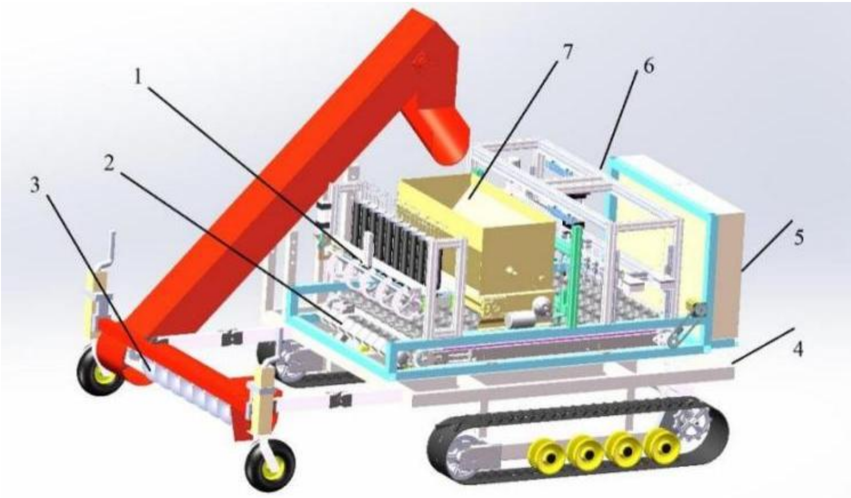

Fig.1 - Schematic diagram of the automatic flower transplanter

1-Soil sampling device; 2-Flowerpot Conveyor System; 3-Soil pickup Device; 4-Frame and Traveling Mechanism; 5-PLC Control Unit; 6-Seedling Transplanting Device; 7-Soil Storage Device

The automatic flower transplanter, shown in Fig. 1, integrates pot separation, substrate filling, hole punching, seedling transplanting, and ridge placement. It consists of a traveling mechanism, a PLC control system, and soil-handling units, enabling the fully automatic transfer of plug seedlings into cultivation pots.

The automatic flower transplanter is equipped with a tracked chassis to provide mobility, with a high-power DC motor serving as the drive unit. During operation, soil is collected and conveyed to the storage unit for uniform filling of soft nursery pots. The operating process is as follows: vacuum suction cups remove pots from stacked racks; the pots are conveyed individually for precise substrate filling; holes are vertically formed in the filled pots; seedlings are transplanted into the holes to ensure close root-soil contact; and finally, the pots are guided into the cultivation ridges through sequential guide plates, thereby achieving uniform placement along the ridges.

DESIGN OF SOIL PICKUP AND SEPARATION DEVICE

Design of Soil pickup and Lifting Unit

The soil pickup and lifting unit consists of a soil lifting box measuring approximately 2100 mm in length and 1800 mm in height after inclined installation, along with a housing, soil-lifting baffle, soil pickup auger, height adjustment mechanism, and soil discharge chute opening as shown in Fig. 2. The chain is positioned at a 40°angle to the ground, with four chain links between adjacent soil-lifting baffles at a pitch of 40 mm. Rotating shaft of the soil pickup auger has a length of 1100 mm and a diameter of 40 mm, while the helical blades feature an outer diameter of 150 mm and a thickness of 2 mm.

The soil pickup auger consists of a rotating shaft and helical blades (*Bulgakov et al., 2023*), while the soil-lifting baffles are composed of steel plates and rigid PVC strips, as shown in Fig. 3. During transplanting operations, the motor drives the auger to rotate and convey soil laterally beneath the baffles. The chain then drives the baffles upward, lifting the soil to the discharge opening.

The soil pickup quantity can be adjusted by changing the engagement length between the externally threaded rocker and the internally threaded square tube. Rotating the rocker outward moves the auger away from the ridge surface, thereby reducing soil pickup, whereas rotating it inward moves the auger closer to the ridge surface, thereby increasing soil pickup.

Design of the Soil Storage and Separation Unit

The soil storage and separation unit (*Li et al., 2019; Feng et al., 2022*) consists of a soil storage box, a conveyor-belt tensioning mechanism, a brushed DC motor, a soil separation quantity adjustment mechanism, a soil separation baffle, a conveyor belt, and a soil separation auger, as shown in Fig. 4. Soil discharged from the chute enters the storage box, is conveyed toward the separation baffle, and is then distributed uniformly into the flowerpots. The soil separation quantity adjustment mechanism, consisting of an adjustment knob, a gear set, and an adjustment plate, changes the gap between the adjustment plate and the conveyor belt by varying the meshing position of the gears, thereby enabling precise soil filling for 10 flowerpots per cycle. The conveyor-belt speed must also be properly adjusted: excessive speed may cause soil accumulation or clogging at the belt-baffle gap, whereas insufficient speed may result in inadequate filling.

Because of structural constraints, the soil discharge chute can only be installed on one side, which may cause soil accumulation near the discharge point. A soil separation auger is therefore used to improve soil conveying and distribution. The auger shaft is supported by F206 bearings and is provided with mounting holes at predetermined intervals, through which the blades are bolted. The shaft has a total length of 955 mm, including an 830 mm conveying section. The mounting holes have a diameter of 15 mm, the blade spacing is 40 mm, and 16 blades are arranged symmetrically around the shaft.

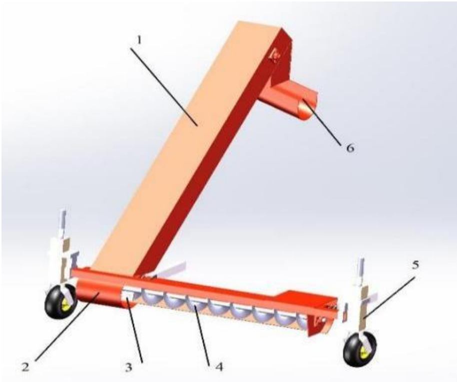

Fig. 2 - Schematic diagram of the soil pickup and lifting unit

1-Soil lifting box; 2-Housing; 3-Soil-lifting baffle; 4-Soil pickup auger; 5-Height adjustment mechanism; 6-Soil discharge chute opening

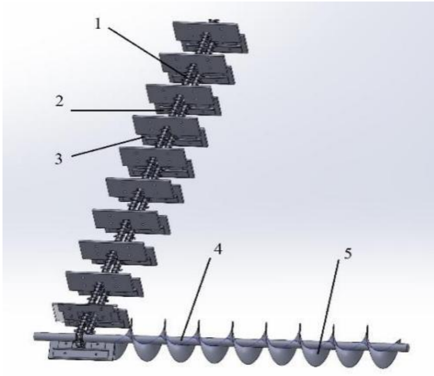

Fig. 3 - Schematic diagram of the soil pickup auger and soil-lifting baffle

1-Chain; 2-Steel plate; 3-Rigid PVC strips; 4-Rotating shaft; 5-Helical blade

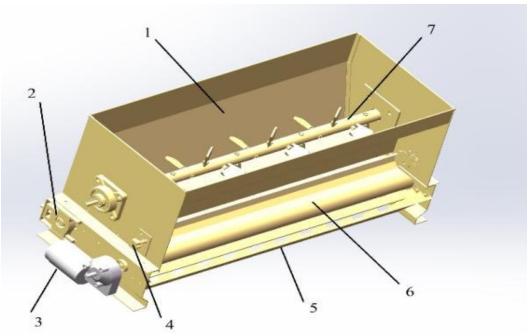

Fig. 4 - Schematic diagram of the soil storage and separation unit

1-Soil storage box; 2-Conveyor belt tensioning mechanism; 3-Brushed DC motor; 4-Soil separation quantity adjustment mechanism; 5-Soil separation baffle; 6-Conveyor belt; 7-Soil separation auger

Analysis of Soil Particle Conveying Characteristics

Soil particles conveyed by the helical blades of the soil separation auger undergo combined axial translation and circumferential rotation. To investigate this motion behavior in detail, the forces acting on individual soil particles and their velocity components during conveying were analyzed using a single-particle analysis method.

Dynamic Analysis

The resultant force F exerted by the helical blade on soil particle P can be decomposed into an axial component F_z along the auger axis and a tangential component F_t. At the same time, particle P is subjected to a normal force F_n from the helical surface and a tangential friction force f_1, as shown in Fig. 5.

Under the combined action of F_t and f_1, P tends to rotate around the auger axis. When F_t is moderate, this rotational tendency is restrained by the combined effects of gravity and the frictional force exerted by the housing. When F_t becomes excessively large, the tendency of particle P to roll increases, thereby reducing the axial conveying efficiency. The force balance of particle P can be expressed by Eq. (1).

$$\begin{cases} F_z = F\cos(\alpha+\beta) \\ F_t = F\sin(\alpha+\beta) \\ f_1 = \mu F_n = F_n \tan\alpha \end{cases} \tag{1}$$

For soil particles to move axially along the auger shaft, the axial driving force must exceed the axial resistance acting on the particles. This condition can be expressed by Eq. (2).

$$\begin{cases} F_n\cos\beta > f_1\sin\beta \\ F_n\cos\beta > F_n\tan\alpha\sin\beta \\ \alpha+\beta < 90^\circ \end{cases} \tag{2}$$

where F is the resultant force exerted by the helical surface on particle P, N; F_n is the normal force exerted by the helical surface N; f_1 is the tangential friction force along the helical surface N; F_z is the axial component of the resultant force along the auger shaft N; F_t is the circumferential component of the resultant force N; α is the friction angle of particle P, °; β is the helix angle of the soil pickup auger °; μ is the sliding friction coefficient between particle P and the helical surface; s is the pitch of the soil pickup auger [mm]; and r is the radial distance from particle P to the auger axis [mm].

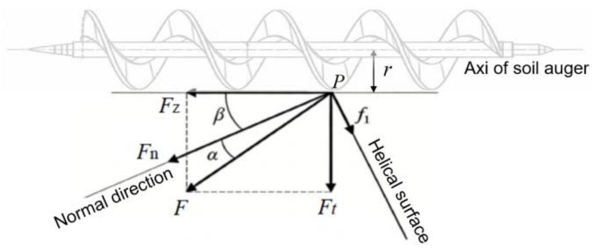

Fig. 5 - Force analysis of a soil particle under the action of the helical blade

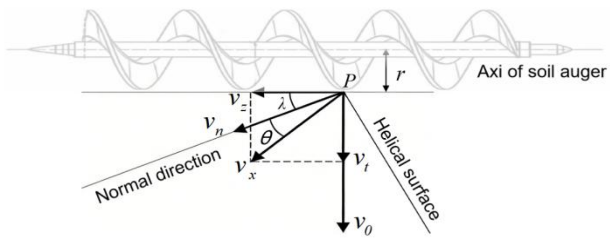

Fig. 6 - Velocity analysis of a soil particle during conveying by the helical blade

<u>Kinematic Analysis</u>

As shown in Fig. 6, the initial velocity of soil particle P is the circumferential velocity V_0 associated with the rotation of the helical blade. If the friction between the particle and the rotating blade is neglected, particle P moves with an absolute velocity V_n along the normal direction of the helical surface. In practice, however, friction causes the actual velocity of particle P to deviate from this direction, resulting in a velocity V_x. This velocity can be decomposed into an axial component V_z along the auger shaft and a circumferential component V_t. The velocity relationships of particle P are given in Eqs. (3) and (4).

$$\begin{cases} V_t = V_x\sin(\alpha+\beta) \\ V_z = V_x\cos(\alpha+\beta) \\ V_0 = wr = \dfrac{2\pi n}{60}r = \dfrac{ns}{60\tan\beta} \\ V_x = \dfrac{V_n}{\cos\alpha} = \dfrac{V_0\sin\beta}{\cos\alpha} = \dfrac{ns\cos\beta}{60\cos\alpha} \end{cases} \tag{3}$$

$$\begin{cases} V_z = \dfrac{ns}{60}(\cos^2\beta - \cos\beta\sin\beta\tan\alpha) \\ V_t = \dfrac{ns}{60}(\cos\beta\sin\beta + \cos^2\beta\tan\alpha) \end{cases} \tag{4}$$

where:

V_x is the actual velocity of particle P considering friction with the rotating blade m/s; V_n is the velocity of particle P along the normal direction of the helical surface m/s; V_0 is the circumferential velocity induced by auger rotation m/s; V_z is the axial velocity component along the auger shaft m/s; V_t is the circumferential velocity component m/s; and n is the rotational speed of the soil pickup auger , rpm.

PERFORMANCE SIMULATION AND OPTIMIZATION OF SOIL PICKUP DEVICE

Transplant Ridge Modeling

Soil samples of 200 g were collected from the ridge surface using the five-point sampling method. The particle size distribution was determined by sieve analysis, showing that particles of 0~1 mm, 1~2 mm, and >2 mm accounted for 70.8%, 14.2%, and 15.0%, respectively. A soil trough of 120 mm (length) × 1250 mm (width) × 200 mm (height) was established in EDEM to simulate the transplanting ridge. To balance simulation efficiency and accuracy, the simulated particle size was set to three times the actual average particle size. Spherical, columnar (three-sphere), and blocky (four-sphere) particles were constructed based on a single sphere with a radius of 3 mm, and generated in the trough according to the measured mass proportions *(Li et al., 2023, He et al., 2024, Huan et al., 2025, Han et al., 2025)*.

Motion Settings for the Soil-Lifting Baffles

A simplified simulation model of the soil pickup and separation device was established in SolidWorks 2022 and imported into EDEM 2023, as shown in Fig. 7. The chain was omitted, and the soil storage unit was simplified as an open box. To simulate the periodic motion of the baffles (*Zhao et al., 2020*), 21 baffles were generated at equal time intervals. Their motion was divided into the following cycle: inclined downward movement → rotation near the auger → inclined upward movement → rotation near the discharge opening → return to the initial position.

Simulation Parameter Settings

The 25s simulation included particle generation and soil filling (0~5.0s), followed by auger rotation and forward movement (5.0~25.0s) with sequential soil lifting. Motion parameters are in Table 1.

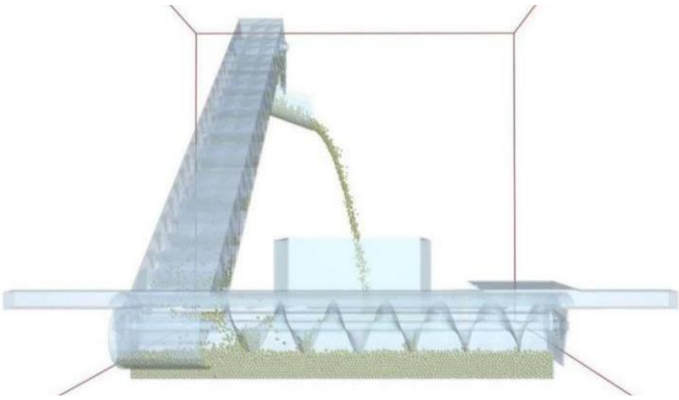

Fig. 7 - EDEM simulation model

Table 1

Motion parameters of the auger shaft and soil-lifting baffles

Auger shaft		Soil lifting baffle	
rotational angular velocity / rad.s^{-1}	13.8	duration of initial inclined descent/s	0.08
forward velocity / m.s^{-1}	0.02	duration of rotation near the auger/s	0.23
		duration of inclined ascent/s	1.56
		duration of rotation near the discharge opening/s	0.23
		duration of return inclined descent/s	1.48
		ascent/descent velocity/m/s	1.2
		rotational angular velocity/rad/s	13.8

Simulation Contact Model and Setting of Material Contact Parameters

Considering the moisture content and cohesiveness of the soil particles, the Hertz–Mindlin with JKR contact model was selected because it can represent the adhesive behavior of moist, cohesive particles under the actual operating conditions of the soil pickup and lifting device (*Han et al., 2023)*. The basic physical property parameters of various materials involved in the study are shown in Table 2, and the contact mechanical property parameters between different materials are presented in Table 3.

Table 2

Physical properties of the materials

Material	Density (kg/m³)	Elastic Modulus (Pa)	Shear Modulus (Pa)	Poisson's Ratio
Soil Particles	1526	$2.808×10^6$	$1.080×10^6$	0.30
Rigid PVC Sheet Strip	1282	$1.056×10^7$	$4.000×10^6$	0.32
Q235 Carbon Steel	7830	$7.270×10^{10}$	$1.963×10^{11}$	0.35

Table 3

Contact parameters between materials

Contact pair	Coefficient of Restitution	Coefficient of Static Friction	Coefficient of Rolling Friction
Soil Particles-Soil Particles	0.45	0.89	0.43
Soil Particles-Q235 Carbon Steel	0.20	0.30	0.03
Soil Particles-Rigid PVC Sheet Strip	0.50	0.50	0.01

Parametric Optimization Simulation Test

To obtain the optimal soil pickup and lifting performance of the device, the operating parameters of the soil pickup auger were optimized, including auger rotational speed, soil penetration depth, and pitch.

Optimization Test Design

To investigate the effects and interactions of the operating parameters of the soil pickup auger, a three-factor, three-level Box-Behnken response surface simulation design was conducted. The coded levels of the experimental factors are presented in Table 4.

Table 4

Coded levels of the experimental factors

Coded level	Test Factor		
	Rotational Speed X_1 ($r.min^{-1}$)	Soil Penetration Depth X_2 (mm)	Pitch X_3 (mm)
-1	90	30	130
0	110	40	150
1	130	50	170

Evaluation Indexes of Optimization Test

The evaluation indices used in the optimization test were the soil lifting quantity, Y_1, and the coefficient of variation of the soil lifting quantity, Y_2. These indices were calculated using Eq. (5).

$$\begin{cases} Y_1 = \dfrac{\sum_{i=1}^{m} x_i}{\phi} \\ Y_2 = \dfrac{\sigma}{Y_1} \times 100\% \\ \sigma = \sqrt{\dfrac{\sum_{i=1}^{m} (x_i - Y_1)^2}{\phi - 1}} \end{cases} \tag{5}$$

where x_1 is the mass of soil in the soil storage box at the i-th measurement kg; ϕ is the number of measurements; σ is the standard deviation of the soil mass in the soil storage box during the simulation; Y_1 is the soil lifting quantity kg; and Y_2 is the coefficient of variation of the soil lifting quantity, %.

RESULTS

Results of Optimization Test

The simulation results of the optimization experiments are presented in Table 5, where X_1 and X_2 represent the coded values of the experimental factors. Multivariate regression fitting and analysis of variance (ANOVA) were conducted on the simulation results of the optimization experiments using Design-Expert 12.0 software, with the results shown in Table 6. The P-values of all models were less than 0.05, indicating that the models were significant and the ANOVA results had high reliability. In addition, the P-values of the lack-of-fit terms were all greater than 0.05, meaning the lack-of-fit terms were not significant and the ANOVA results had a high degree of fitting. For the response surface model of soil lifting quantity, Y_1, the terms X_1, X_2, X_1X_2, X_1X_3, X_2^2 and X_3^2 had highly significant effects on the response, while X_3 and X_2X_3 had significant effects. For the response surface model of the coefficient of variation of soil lifting quantity Y_2, the terms X_1, X_2, X_3, X_1X_2, X_1X_3 and X_1^2 had highly significant effects, and X_3^2 had a significant effect.

Table 5

Box-Behnken design and simulation results

Serial Number	Test Factor			Evaluation Index	
	X_1	X_2	X_3	Y_1/kg	Y_2/%
1	-1	-1	0	2.73	1.16%
2	1	-1	0	4.31	1.77%
3	-1	1	0	4.85	1.27%
4	1	1	0	5.51	1.42%
5	-1	0	-1	4.05	1.30%
6	1	0	-1	4.52	1.85%
7	-1	0	1	3.52	1.17%
8	1	0	1	4.93	1.44%
9	0	-1	-1	3.78	1.72%
10	0	1	-1	5.65	1.55%
11	0	-1	1	3.75	1.46%
12	0	1	1	5.17	1.44%
13	0	0	0	4.18	1.50%
14	0	0	0	4.28	1.52%
15	0	0	0	4.13	1.44%
16	0	0	0	4.19	1.50%
17	0	0	0	4.23	1.49%

Table 6

ANOVA for the response surface models

Source of Variance	Soil Lifting Quantity				Coefficient of Variation of Soil Lifting Quantity			
	SS	df	F-Value	P-Value	SS	df	F-Value	P-Value
Model	8.49	9	137.48	< 0.0001**	0.0231	1	20.29	0.0028**
X_1	2.12	1	309.40	< 0.0001**	0.1035	1	90.86	< 0.0001**
X_2	5.46	1	796.39	< 0.0001**	0.0529	1	46.43	0.0002**
X_3	0.0496	1	7.23	0.0311*	0.0196	1	17.20	0.0043**
X_1X_2	0.2116	1	30.86	0.0009**	0.0056	1	4.94	0.0617
X_1X_3	0.2209	1	32.21	0.0008**	0.0370	1	32.48	0.0007**
X_2X_3	0.0506	1	7.38	0.0299*	0.0003	1	0.2830	0.6112
X_1^2	0.0358	1	5.22	0.0562	0.0081	1	7.07	0.0325*
X_2^2	0.2430	1	35.44	0.0006**	0.0231	1	20.29	0.0028**
X_3^2	0.0888	1	12.95	0.0088**	0.1035	1	90.86	< 0.0001**
Residual	0.0480	7			0.0080	7		
Lack of Fit	0.0353	3	3.71	0.1187	0.0044	3	1.62	0.3185
Pure error	0.0127	4			0.0036	4		
Total	8.53	16			0.5683	16		

Note: **: P<0.01 (indicates a highly significant effect); *: P<0.05 (indicates a significant effect); no symbol: *P*>0.05 (indicates not significant).

With the model significance guaranteed and the lack-of-fit terms confirmed to be non-significant, the non-significant terms for the response were eliminated, and the optimized regression equations for soil lifting quantity Y_1 and the coefficient of variation of soil lifting quantity Y_2 were obtained as follows:

$$Y_1 = 7.70 + 0.5150 x_1 + 0.8263 x_2 - 0.0788 x_3 - 0.2300 x_1 x_2 + 0.2350 x_1 x_3 - 0.1125 x_2 x_3 + 0.2402 x_2^2 + 0.1453 x_3^2 \quad (6)$$

$$Y_2 = 1.49 + 0.1975 x_1 - 0.0538 x_2 - 0.1138 x_3 - 0.1150 x_1 x_2 - 0.0700 x_1 x_3 - 0.0937 x_1^2 + 0.0437 x_3^2 \quad (7)$$

The results of analysis of variance (ANOVA) indicated that the coefficients of determination (R_1^2=0.9944, R_2^2=0.9860) and adjusted coefficients of determination (R_1^2adj=0.9871, R_2^2adj=0.9679) of the fitted models all approached 1.00, which demonstrated that the regression models possessed an extremely high fitting accuracy and strong correlation.

Interaction Analysis of the Regression Models

To investigate the effects of the interaction between the experimental factors on the soil lifting quantity Y_1 and its coefficient of variation Y_2, response surface analysis was performed on the ANOVA results of the optimization experiments via Design-Expert 12, as shown in Fig. 8.

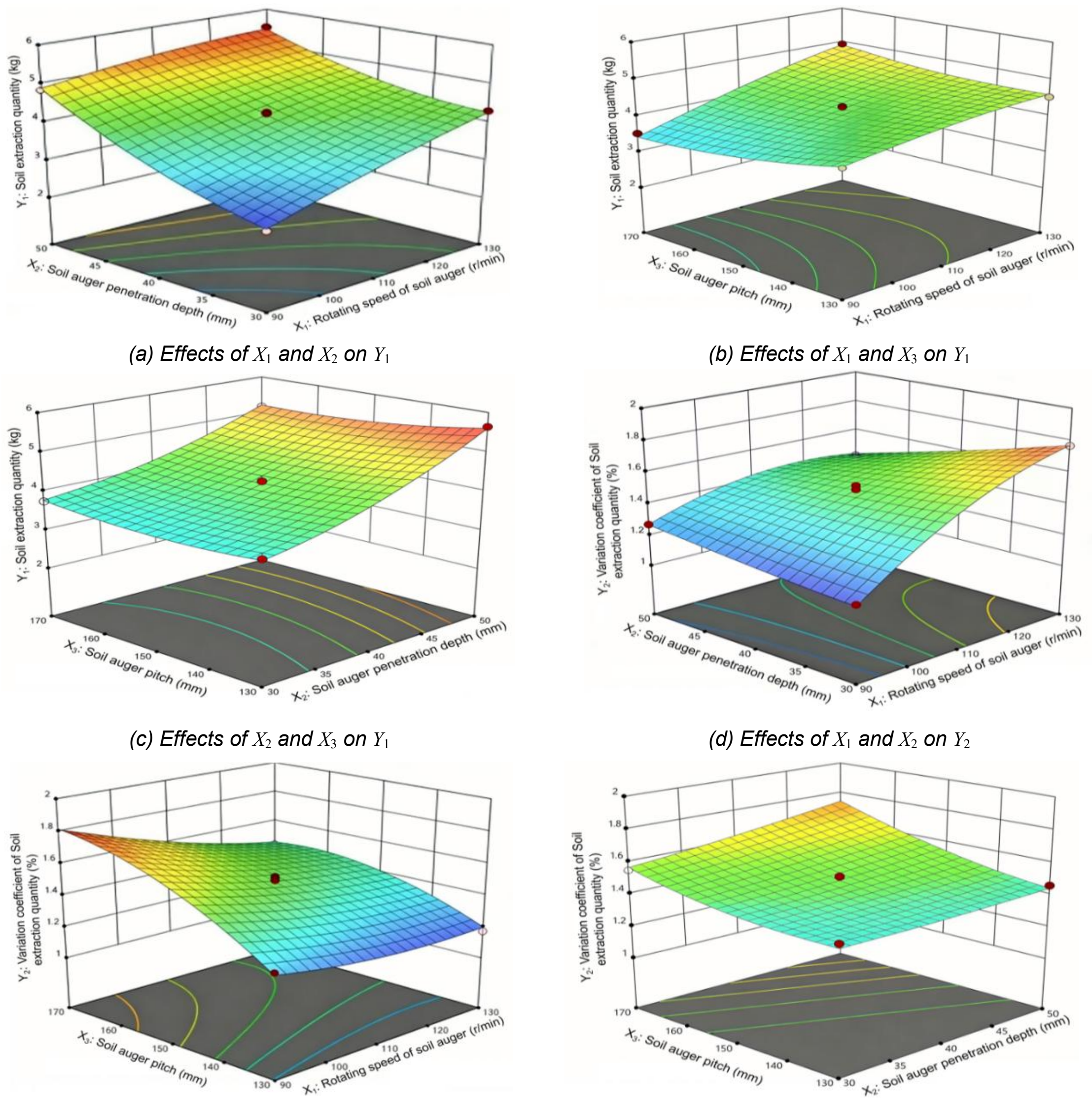

(a) Effects of X_1 and X_2 on Y_1

(b) Effects of X_1 and X_3 on Y_1

(c) Effects of X_2 and X_3 on Y_1

(d) Effects of X_1 and X_2 on Y_2

(e) Effects of X_1 and X_3 on Y_2

(f) Effects of X_2 and X_3 on Y_2

Fig. 8 - Effects of the experimental factors on soil lifting quantity and its coefficient of variation

As shown in Fig. 8(a), Y_1 increased gradually with increasing rotational speed and increased sharply with increasing soil penetration depth, indicating that soil penetration depth had the greater effect. As shown in Fig. 8(b), Y_1 increased continuously with increasing rotational speed, while changes in pitch had only a slight effect, indicating that rotational speed was the more influential factor. As shown in Fig. 8(c), Y_1 increased markedly with increasing soil penetration depth and changed only slightly with pitch, confirming that soil penetration depth had the greater effect. As shown in Fig. 8(d), Y_2 increased sharply with increasing rotational speed but only gradually with increasing soil penetration depth, indicating that rotational speed had the stronger effect. As shown in Fig. 8(e), Y_2 increased rapidly with increasing rotational speed and remained nearly unchanged with changes in pitch, indicating that rotational speed was the dominant factor.

As shown in Fig. 8(f), Y_2 decreased gradually with increasing soil penetration depth and also decreased with increasing pitch, indicating that soil penetration depth had the greater influence. Overall, the response surface analysis indicates that the interaction between rotational speed and soil penetration depth has an important effect on soil lifting performance, which is consistent with the ANOVA results.

Optimal Parameter Combination

To ensure that the soil lifting quantity met the requirements of practical operation while maximizing the stability of the soil lifting process, the operating parameters were optimized. The optimal parameter combination was an auger rotational speed of 116 rpm, a soil penetration depth of 40 mm, and a pitch of 150 mm. Three repeated simulation validation tests were conducted, and the mean values were used to evaluate the optimization results. The resulting soil lifting quantity, Y_1, was 4.26 kg, and the coefficient of variation of soil lifting quantity, Y_2, was 1.50%. These values were in good agreement with the predicted optimization results.

FIELD TRIALS

Test Conditions

The field trials were conducted at the experimental field of Rongliang Ecological Agriculture Co., Ltd. in Heishan County. A laser tachometer was used to adjust the auger rotational speed, an electronic balance was used to measure the soil lifting quantity, and a tape measure was used to evaluate ridge flatness. The field test procedure is shown in Fig. 9(a).

(a) Soil Pickup Process **(b) Selection of Measurement Sections** **(c)Surface Levelness Measurement**

Fig. 9 - Field test

Test Methods and Content

The experimental design methodology and measurement procedures were based on the preceding simulation tests and relevant literature. To enhance the reliability of field trial data and comprehensively evaluate the performance of the soil pickup device, which the surface levelness Y_3 was measured. Manual measurement methods were employed, with a tape measure used to select one measurement section every 3 meters along the transplanted ridges. The vertical distance from the surface of randomly sampled points, which each measurement section to the reference plane was measured, it is shown in Figs. 9(b) and 9(c).

The primary evaluation metrics for the tests include soil lifting quantity, coefficient of variation for soil lifting quantity, and surface levelness. Each test group was replicated three times, with calculations performed according to Equations (8).

$$Y_3 = \sqrt{\frac{\sum_{j=1}^{n}\left(a_{kj}-a_k\right)^2}{n_k-1}} \tag{8}$$

where n_k represents number of test points in the k-th measurement; a_{kj} represents measure the vertical distance from the ground surface to the horizontal reference line before and after the k-th measurement at the j-th equidistant point, mm; a_k represents vertical distance from the ground surface to the horizontal reference line before and after the k-th soil pickup operation, mm; Y_3 represents surface levelness, mm.

Experimental Results and Analysis

Three suboptimal parameter combinations closely resembling the optimal operating parameter combination were selected from Table 5. Each combination underwent three replicate trials, with results averaged. The field trial outcomes are presented in Table 7.

Table 7

Field experiment results

Group Number	Rotational speed	Soil penetration depth	Pitch	Soil lifting quantity/ kg	Coefficient of variation of soil lifting quantity/ %	Surface levelness / mm
1	130	30	150	4.35	1.82	110
2	90	50	150	5.03	1.55	90
3	130	40	130	4.66	1.61	100
4	116	40	150	4.13	1.44	100

The field test results showed that, under the optimal operating parameter combination determined from the simulation, the soil lifting quantity, Y_1, was 4.13 kg and the coefficient of variation of soil lifting quantity, Y_2, was 1.44%. Compared with the simulation results, the relative errors were only 3.05% and 4.00%, respectively. Under the same parameter combination, the surface levelness, Y_3, was approximately 100 mm. The close agreement between the field test and simulation results verifies the accuracy and reliability of the numerical simulation model.

CONCLUSIONS

A soil pickup and separation device for an automatic flower transplanter was designed in this study. The structural parameters of the key components were determined, and the soil-conveying characteristics of the helical blades of the soil pickup auger were analyzed.

Through parameter optimization based on simulation, the optimal operating parameters were determined as follows: auger rotational speed of 116 rpm, soil penetration depth of 40 mm, and pitch of 150 mm. Under these conditions, the simulated soil lifting quantity, Y_1, was 4.26 kg, and the coefficient of variation of soil lifting quantity, Y_2, was 1.50%.

Field tests conducted under the optimal operating conditions yielded a soil lifting quantity of 4.13 kg and a coefficient of variation of 1.44%. The relative errors compared with the simulation results were 3.05% and 4.00%, respectively. The measured surface levelness, Y_3, was approximately 100 mm. The close agreement between the simulation and field test results indicates that the structural design and numerical model are reliable. The device can meet the soil-handling requirements of automatic flower transplanting operations and provides a basis for its further application in greenhouse production.

ACKNOWLEDGEMENT

This research was supported by Liaoning Provincial Department of Agriculture and Rural Affairs - “Xingliao Talent Program” Agricultural Expert Project (Grant No. XLYC2413011).

REFERENCES

[1] Bulgakov, V., Kaletnik H., Trokhaniak O., Lutkovska S., Klendii M., Ivanovs S., Popa L., Yaropud V. (2023). Investigation of the Energy Indicators for the Surface Treatment of Soil by a Harrow with a Screw-Type Working Body. *INMATEH--Agricultural Engineering*, 71(3), 818-833. DOI: 10.35633/inmateh-71-72.

[2] Cheng, T., Wang, J., Zheng, T., & Zhang, Q. (2023). From "Mother of Gardens" to "Beautiful China" (从“花园之母”到“美丽中国”). *Chinese Landscape Architecture*, 39 (6), 107-113.

[3] Feng, X., Chen, L., Li, M., & Xiang, J. (2022). Design and Test of Potato Soil Separation Device Based on Potato Harvester (基于土豆收获机的土壤分离装置的设计与测试). *ACM International Conference Proceeding Series*, 135-142.

[4] Gu, Z. (2025). China's seedling and flower enterprises achieve an annual output value exceeding 520 billion yuan (中国种苗花卉企业年产值超 5200 亿元). *People's Daily*, 03-22 (002).

[5] Han, D., Hu, J., Liu, H., Ren, L., Zhou, M., Yang, Q., Li, B., & Chen, X. (2025). Parameter calibration and experiment of the discrete element contact model of water-containing sandy soil particles (含水砂土颗粒离散元接触模型的参数校准与实验). *Nongye Gongcheng Xuebao/Transactions of the Chinese Society of Agricultural Engineering*, 41(8), 70-78. DOI: 10.11975/j.issn.1002-6819.202407112.

[6] He, L., Jiang, J., Li J., Zhang, F., Yi, S., Zheng, Y., & Lv, Q. (2023). Design and test of seedling pot filling and hole punching processing line for citrus (柑橘育苗钵装填成穴生产线的设计与试验). *Journal of Southwest University (Natural Science Edition)*, 45 (5), 108-121. DOI: 10.13718/j.cnki.xdzk.2023.05.011.

[7] He, X., Ma, S., Liu, Z., Wang, D., Shang, S., Li, G., & Li, H. (2024). Calibration and testing of saline soil parameters based on EDEM discrete element methodology (基于 EDEM 离散元方法的盐碱土壤参数标定与测试). *INMATEH - Agricultural Engineering*, 73(2), 822-833. DOI: 10.35633/inmateh-73-69.

[8] Hu, J., Liu, Y., Liu, W., et al. (2022). Experiment on Combined Seedling Picking Device with Top Clamping and Pulling (蔬菜自动移栽机顶夹拔组合式取苗装置试验研究). *Transactions of the Chinese Society for Agricultural Machinery*, v53, p110-117. DOI: 10.6041/j.issn.1000-1298.2022.S1.013.

[9] Huan, X., Feng, M., Wu, C., Jia, J., & Chen, J. (2025). Construction and Experiment of Discrete Element Model for Tea Garden Soil-Organic Fertilizer Mixture Based on EDEM (基于 EDEM 的茶园土壤-有机肥混合物离散元模型的构建与试验). *Nongye Jixie Xuebao / Transactions of the Chinese Society for Agricultural Machinery*, 56(12), 267-278. DOI: 10.60465/j.issn.1000-1298.2025.12.024.

[10] Ji, D., Hu, X., Zhe, X., Bia, X., Gong, Y., & Tian, S. (2022). Design and experiment of double row transplanting manipulator linkage high speed transplanting device (双排移栽机械手联动式高速移栽装置设计与试验). *Transactions of the Chinese Society for Agricultural Machinery*, 52 (12), 126-133, 146. DOI:10.6041/j.issn.1000-1298.2022.12.012.

[11] Li, B., & Gao, G. (2019). Research on parameter optimization of potato soil transportation separation mechanism (土豆土壤运输分离机构参数优化研究). *Proceedings - 2019 2nd World Conference on Mechanical Engineering and Intelligent Manufacturing*, WCMEIM 2019, 147-150.

[12] Li, S., Diao, P., Zhao, Y., Miao, H., Li, X., & Zhao, H. (2023). Calibration of discrete element parameter of soil in high-speed tillage (高速耕作条件下土壤离散元标定). *INMATEH - Agricultural Engineering*, 71(3), 248-258. DOI: 10.35633/inmateh-71-21.

[13] Minglani, D., Sharma, A., Pandey, H., Dayal, R., & Joshi, J. (2021). Analysis of flow behavior of size distributed spherical particles in screw feeder. *Powder Technology*, v382, p1-22. DOI: 10.1016/j.powtec.2020.12.041.

[14] Tian, S., Hu, X., Xie, T., Zhe, X., Li, B. & Sun, Z. (2022). Design and experimental study on automatic separation device for multiple stacked seeding bowls (多组叠摞营养钵同时自动分离装置设计与试验). *Journal of Shenyang Agricultural University*, 53 (01),103-109. DOI: 10.3969/j.issn.1000-1700.2022.01.013.

[15] Tian S., Xie, T., Wang H., Zhang, X., Zhang, K., Bai, X., & Sun, Z. (2023). Design and experiment of adjustable seedling-feeding device for vegetable transplanting machine (蔬菜移栽机可调式喂苗装置设计与试验). *Journal of South China Agricultural University*, 44 (3), 464-472. DOI: 10.7671/j.issn.1001-411X.202205012.

[16] Tong, J., Shang, K., Wang, X., Sun, L., Zhang, N., NORUPIRI, R., & Man, S. (2024). Design and Test of Spiral Rejection Mechanism for Inferior Bowl Seedlings (温室穴盘育苗劣质钵苗螺旋式剔除机构设计与试验). *Transactions of the Chinese Society for Agricultural Machinery*, 55 (9), 129-137. DOI: 10.60465/j.issn.1000-1298.2024.09.013.

[17] Xu, Q., Li, S., Zhang, Y., Meng, L., Lu, H., & Xie, L. (2020). Design and test of seedling pot filling and transporting machine for citrus (柑橘育苗钵装填转运机设计与试验). *Transactions of the CSAE*, 36 (18), 66-72. DOI: 10.11975/j.issn.1002-6819.2020.18.009.

[18] Zhao, R., Guo, L., Gao, W., & Xiao, X. (2022). Structure Optimization Design of Screw Conveyor based on EDEM (基于 EDEM 的螺旋输送机结构优化). *Journal of Physics: Conference Series*, 2200(1). DOI: 10.1088/1742-6596/2200/1/012002.

[19] Zhao, X., Guo, J., Li, K., Dai, L., & Chen, J. (2020). Optimal design and experiment of 2-DoF five-bar mechanism for flower seedling transplanting (花卉苗移栽二自由度五杆机构的优化设计与试验). *Computers and Electronics in Agriculture*, 178, 105746. DOI:10.1016/j.compag.2020.105746.

[20] Zhao, X., Zhang, X., Wu, Q., Dai, L., & Chen, J. (2020). Research and experiment of a novel flower transplanting device using hybrid-driven mechanism (基于混合驱动机构的新型花卉移栽装置研究与试验). *International Journal of Agricultural and Biological Engineering*,13 (2), 92-100. DOI: 10.25165/j.ijabe.20201302.5187.

[21] Zhou, M., Xu, J., Tong, J., Yu, G., Zhao, X., & Xie, J. (2018). Design and experiment of integrated automatic transplanting mechanism for taking and planting of flower plug seedlings (花卉穴盘苗取栽一体式自动移栽机构设计与试验). *Transactions of the CSAE*, 34 (20), 44-51. DOI: 10.11975/j.issn.1002-6819.2018.20.006.